MERCK

catch the SUN

Product Category list:

- Organic Photovoltaic (OPV) Donors and Acceptors
- Dye-Sensitized Solar Cell Materials
- Perovskite Materials

Visit us at:
SigmaAldrich.com/organic-electronics

MK_AD9792EN 43729 08/2022

The Life Science business of Merck operates as MilliporeSigma in the U.S. and Canada.

Sigma-Aldrich®
Lab & Production Materials

ADVANCED ENERGY MATERIALS
www.advenergymat.de

Ionic Organic Thermoelectrics with Impressively High Thermopower for Sensitive Heat Harvesting Scenarios

Ya-Hsin Pai, Junhui Tang, Yan Zhao, and Ziqi Liang**

As the worldwide energy crisis is worsened, thermoelectric materials that can harvest low-grade waste heat and directly convert it into electricity provide promising alternative energy sources. Emerging ionic thermoelectrics (iTEs) have recently attracted widespread attention thanks to their impressively high thermopower that can reach hundreds of times more than conventional electronic thermoelectrics (eTEs). Based on the Soret effect, the performances of iTEs depend on the thermo-diffusion of mobile ions in electrolytes, resulting in electrical characteristics distinct from eTE materials and opening up additional potential applications of thermoelectrics. Among these materials, organics-based iTEs (i-OTEs) provide unique advantages such as low-cost, light-weight, and eco-friendliness, thereby offering more promising application scenarios that can utilize dissipated heat, for example, from human bodies or mobile devices. This concise review begins with the comparison of iTE and eTE, and then discusses their different mechanisms and applied devices in detail. Next, the recent advances of i-OTEs will be in-depth highlighted, including the merits and weaknesses of representative types of materials, effects of additives, and effective strategies for performance optimization. Finally, the state-of-the-art achievements of i-OTEs are summarized, and an overview is provided of the existing challenges and an outlook of prospective development and applications in future efforts.

1. Introduction

Thermoelectric technology is regarded as a facile solution to convert low-grade waste heat into electricity, which is conducive to mitigating energy crises worldwide. Electronic thermoelectrics (eTEs) have been investigated for decades and shown good prospects in small-scale thermoelectric generators (TEGs) and cooling devices, yet their thermovoltages have almost approached a certain limit, hindering further large-scale applications.[1–3] Ionic thermoelectrics (iTEs) have recently emerged, on the other hand, and likewise can generate potential differences between electrodes from absorbed heat yet with the induced thermopower much higher than any eTE materials can reach. iTEs are based on the Soret effect, whose performances are solely dependent on the thermo-diffusion of ions in electrolytes, whereas eTEs are built on the diffusion of holes or electrons induced by temperature gradient, which is known as Seebeck effect. Such a key mechanistic disparity affords the applications of iTEs different than eTEs, the former of which must be in a supercapacitor form since the ions would be blocked by interfaces between electrolyte and external electrodes, in stark difference from TEGs of the latter.

Typical iTE materials include inorganic ionic solids, liquids, and conducting polymers as well as polyelectrolytes, which have been well-studied in recent years. Among them, inorganic materials are cost expensive, environmentally harmful, and mechanically rigid, whereas organic analogs are solution-processable, light-weight, mechanically flexible and stretchable, and eco-friendly, thereby becoming a better candidate for applications in portable or wearable electronic devices. An active quest for favorable organic-based materials with outstanding iTE performance currently constitutes a prime research direction. In this scenario, ionic organic thermoelectric (abbreviated as i-OTE) materials have now attracted increasing attention thanks to their impressively high thermopowers, which hold great potential to meet the demands of higher voltage output in thermal-sensitive sensors, for instance.

As iTEs have developed rapidly in recent years, their basic principles and mechanisms have been detailed in few articles, representative of Yu, Crispin and Ouyang groups.[4–6] In this Review, we will in particular center on organic thermoelectric materials with numerous advantages as mentioned earlier, and outline the historical development of i-OTEs by beginning with a comparison of ionic and electronic OTEs with regards to the mechanisms, merits/shortcomings, and applications. An in-depth discussion of recent advances in materials and potential applications in i-OTEs will be followed. A conclusion with significant hurdles on further developments and a perspective with promising avenues will be presented.

Y.-H. Pai, J. Tang, Y. Zhao, Z. Liang
Department of Materials Science
Fudan University
Shanghai 200433, China
E-mail: zhaoy@fudan.edu.cn; zqliang@fudan.edu.cn

The ORCID identification number(s) for the author(s) of this article can be found under https://doi.org/10.1002/aenm.202202507.

DOI: 10.1002/aenm.202202507

2. Ionic versus Electronic Thermoelectrics

2.1. Mechanism: Soret Effect and Seebeck Effect

Conventional eTEs are based on the Seebeck effect, named after the first founder Thomas Seebeck in 1821. The temperature difference between two conductors connected in series would develop an electromotive force, quantified with the Seebeck coefficient (S):

$$S = \frac{V}{\Delta T} \tag{1}$$

where ΔT is the temperature difference, and V is the induced open-circuit electromotive force.[7–10] S generally depends on the charge carrier diffusion, which drives free carriers to move toward the cold side of materials. Thus, semiconductor materials with a majority of hole carriers possess a positive S, defined as p-type materials, and the hot side has a lower voltage; likewise, those with a majority of electron carriers show a negative S, defined as n-type materials, and the cold side has a lower voltage. According to theoretical analysis, the performance of eTEs, including the maximum output power (P_{max}) of generators, temperature differences (ΔT_{max}) and cooling capacities ($Q_{c,max}$) of coolers, are all dependent on the Seebeck coefficient, electrical and thermal conductance of materials.[11] Thus, the dimensionless thermoelectric figure of merit $zT_e = S^2\sigma T/\kappa$ is introduced to evaluate the performance of materials, where σ and κ are the electrical and thermal conductivities, respectively.

For an iTE material, the thermopower is generated by thermodiffusion of mobile cations or anions, which serve as charge carriers in ionic systems. The basic of iTEs is the Soret effect, discovered by Charles Soret in 1879, which was first referred to the nonuniform salt concentration in an electrolyte solution between two ends with different temperatures. In 1926, the heat of transport (Q^*) was introduced by Eastman to estimate the slight temperature change of a particle while transporting between two regions. In this fashion, the ionic thermopower (α) of an iTE can be likewise derived from Equation 1, which can theoretically be derived from the difference in the heat of transport between cations and anions as shown in Equation 2:

$$\alpha = \frac{t_+Q_+^* - t_-Q_-^*}{Te} \tag{2}$$

weighted with the Hittorf ion transport numbers $t_\pm = c_\pm\mu_\pm/(c_+\mu_+ + c_-\mu_-)$, and c and μ are the concentration and mobility of ions. According to Equation 2 and the concept of Q^*, the α of iTE materials mainly depends on the transport properties of ions, which is analogous to the S of eTE materials.[4–6]

Similarly, the performances of iTE can be expressed by the dimensionless ionic figure of merit

$$zT_i = \frac{\sigma_i\alpha^2}{\lambda}T \tag{3}$$

where σ_i and λ are the ionic electrical and thermal conductivities, respectively. Since the efficiency of an ionic thermoelectric supercapacitor (ITESC) is dependent on the zT_i of iTE materials,[12–14] which will be discussed later, an optimization of zT_i values remains a main target in the development of iTEs as well as eTEs.

2.2. Merit and Weakness

Despite both the S and σ of eTEs have been improved throughout these years, the S of electronic OTEs (namely e-OTEs) seems to reach its limit that ranges from 10^{-2} to 10^{-1} mV K^{-1} for most conductive organic small molecules and polymers.[2,15,16] That is why i-OTEs have attracted increasing attention since they were first reported in 2015;[17] the most noticeable advantage of i-OTEs is the ultra-high thermopower, which can reach a few mV K^{-1} or even higher. By virtue of such outstanding features, i-OTEs have shown their great potential to be applied in devices that need higher voltage outputs, such as delicate temperature sensors with better thermal sensitivity.

Even so, some disadvantages of iTEs have yet to be overcome. Most reported electrolytes for iTE have ionic conductivities (σ_i) much lower than the electrical conductivities (σ) of eTEs. For highly doped organic materials, the σ values usually fall within a range of 10^2–10^3 S cm^{-1},[2,15] while the σ_i of i-OTE materials are far below 1 S cm^{-1}, typically within 10^{-3}–10^{-2} S cm^{-1} for most of the electrolytes.[6,17,18] This weakness hinders the probability of i-OTE reaching a higher zT_i value and thus the device efficiency that depends on the zT_i value of materials will be relatively low.

Since ionic charge carriers in the iTE system are unable to pass through the interface between electrolytes and electrodes,[12,19] the generated 'electricity' cannot transfer to external circuits when connected. To utilize the electric potential generated by i-OTE systems, the devices must be built in a supercapacitor form by applying a four-stage operating procedure. This therefore becomes more complicated than a conventional electronic TEG and is hard to generate a steady, continuous output power for practical applications.

2.3. Applications

For conventional eTEs, power generators and refrigerators are two most common applications. The basic structure of a thermoelectric device is p-n junctions connected electrically in series and thermally in parallel. As shown in **Figure 1**a, in the power generator mode, a temperature difference is applied between two ends of p-n legs, and the generated electricity can be output to an external circuit. In the cooling mode, the applied current makes external heat absorbed by the cold sides.[10] Organic materials have been involved in many experimental devices and shown their great potential for wearable devices with their intrinsic flexibility and stretchability.[2,16,20] However, since the relatively low zT_e values of organic materials would lead to poor efficiency of cooling devices, few organic materials have been successfully applied in thermoelectric cooling devices.

As discussed above, iTEs cannot be applied in the conventional generator but has to be designed into a capacitor form. The operation of an ITESC is schematically shown in Figure 1b, which includes the following four stages:[5,12,13] i) *Thermo-ionic charging stage*. It is driven by the temperature gradient, cations and anions are separated and accumulated at the two electrodes, creating potential in electrolytes between the hot and cold sides of the ITESC. ii) *Forward electronic working stage*. An external load is connected with the ITESC,

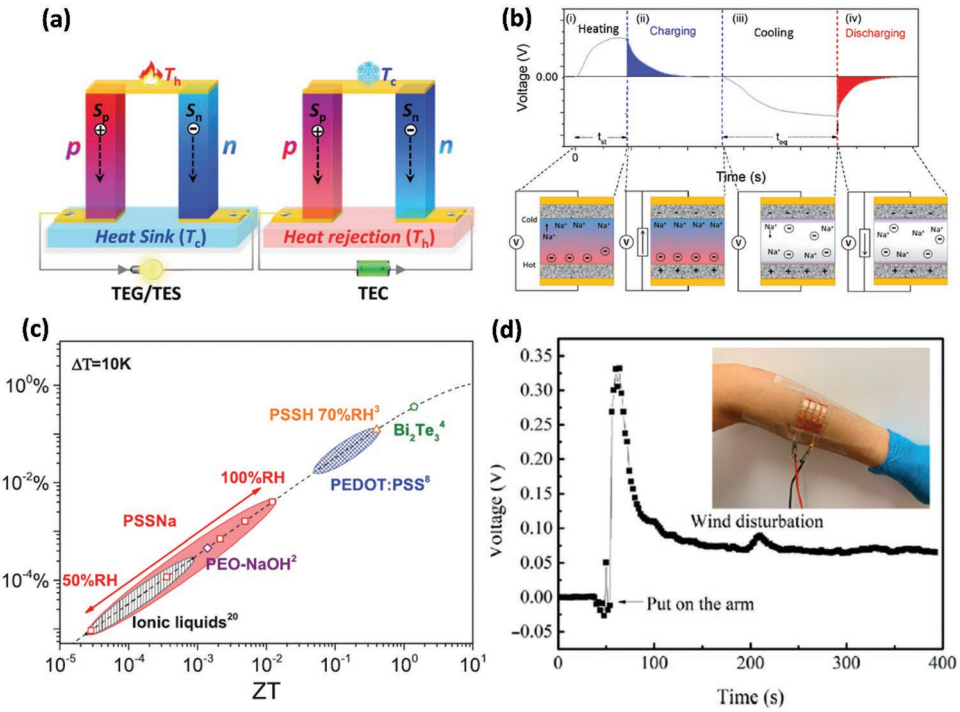

Figure 1. a) Schematic illustration of the eTE uni-couples operation processes used for thermoelectric generators (TEGs) and thermoelectric coolers (TECs). Reproduced with permission.[10] Copyright 2021, Royal Society of Chemistry. b) Operation principle of ionic thermoelectric supercapacitor (ITESC). c) The efficiencies of materials with different *zT*. Reproduced with permission.[12] Copyright 2017, Wiley-VCH. d) Voltage generated from the ionic thermoelectric device when put on a human arm at 25 °C. Reproduced with permission.[29] Copyright 2022, American Association for the Advancement of Science.

in which electrons flow through the external load and balance the potential between the two electrodes. iii) *Thermo-ionic discharging stage*. The temperature gradient is removed and the external load is disconnected, and cations and anions are retrieved and dispersed in the electrolyte. iv) *Reverse electronic working stage*. An external load is re-connected to the ITESC, and electrons are drawn back to balance the inverse potential. The current flow in the opposite direction to that at stage (ii). The ions accumulated at the interfaces between electrolyte and electrodes create a voltage difference, which can drive a current flow in the external circuit, realizing the heat-to-electricity conversion from iTE materials. As a result, by switching the connection of external load and the temperature gradient, the energy can be harvested and utilized in both (ii) and (iv) stages in this typical thermocycle.

ITESCs consisting of i-OTE electrolytes naturally inherit the advantage of high thermopower. For example, the Horike group reported an overall α of 37 mV K^{-1} for an ITESC with five p-type 1-ethyl-3-methylimidazolium chloride (EMIM-Cl)/polyvinyl alcohol (PVA) elements connected in series.[21] Crispin et al. fabricated an ITESC with 18 1-ethyl-3-methylimidazolium bis(trifluoromethylsulfonyl) imide (EMIM-TFSI)/poly(vinylidene fluoride-hexafluoropropylene) (PVDF:HFP) p-n pairs, which reached an α of 333 mV K^{-1}.[22] By comparison, traditional eTEs such as inorganic Bi_2Te_3 and organic PEDOT:PSS only produce at most several hundred μV K^{-1} per unit pair,[9,23,24] which would therefore require hundreds or thousands of legs to match the thermopower provided by an ITESC with few legs. In addition, it is worth noting that the materials chosen for electrodes are also important factors influencing the performance of ITESCs. For instance, the interactions between electrodes and electrolytes through the interfaces can markedly affect the behavior of output voltage,[21,25] for which higher surface area can also effectively increase the capacity of an ITESC.[13,26,27] Detailed discussion about electrodes materials can be found later in Section 3.3.

With the impressively high thermopower and the intrinsically low thermal conductivity,[22] the four-stage operation of ITESCs is able to realize the much low-grade heat harvesting as the eTE generators can. However, the uncompetitive efficiency of devices remains a sharp weakness of i-OTEs. The theoretical maximum efficiency (η) of an ITESC can be expressed as

$$\eta = \frac{2\Delta T}{T_H} \frac{zT_i}{2zT_i + \frac{10T}{T_H} - \frac{1}{2}zT_i\frac{\Delta T}{T_H}} \quad (4)$$

In comparison, the maximum efficiency for a traditional electronic thermoelectric generator (TEG) is

$$\Phi_{max} = \frac{\Delta T}{T_H} \frac{\sqrt{1+zT_e}-1}{\sqrt{1+zT_e}+\frac{T_C}{T_H}} \quad (5)$$

which means that ITESCs with materials of much lower zT_i resulted from poor ionic conductivities are currently unable to reach a satisfying efficiency as high as classic TEGs (Figure 1c).[12–14]

Table 1. Comparison of ionic and electronic organic thermoelectrics.

	Electronic OTEs	Ionic OTEs
Mechanism	Seebeck effect	Soret effect
Charge Carrier	hole/electron	cation/anion
Materials	Semiconducting organic small molecules/polymers	Ionic liquids, ionic polymers
Thermopower	10^{-2}–10^{-1} mV K^{-1}	1–40 mV K^{-1}
Electrical/Ionic Conductivity	10^{2}–10^{3} S cm^{-1}	10^{-3}–10^{-2} S cm^{-1}
Thermal Conductivity	$0.1 < \kappa < 1$ W m^{-1} K^{-1}	$0.1 < \lambda < 1$ W m^{-1} K^{-1}
Advantages	• Transportation of carriers across electrodes into an external circuit	• High thermopower
Weaknesses	• Low output voltage	• Low ionic electrical conductivity • Unsuitable for continuous operation of traditional TEGs
Prospect Applications	• Thermoelectric generators (TEGs) • Thermoelectric coolers (TECs)	• Ionic thermoelectric charged supercapacitors (ITESCs) • Thermal sensors

Another potential application of i-OTEs lies in wearable thermal sensors. The high thermopowers of iTE materials lead to significant potential differences between electrodes with small temperature gradients, which can be applied to a more sensitive thermal sensor. The devices directly utilize the output voltage as the signal, which has more straightforward fabrication and operation procedures than an ITESC. In this respect, Zhang and Huang et al. developed sensors based on i-OTE materials, which are light-weight and flexible so that they can be adhered to human skin, and a small temperature difference, even a wind disturbing, can be sensed and recorded (Figure 1d).[28,29]

In sum, a comparison between e-OTEs and i-OTEs is explicitly presented in **Table 1**. Despite that ions in electrolytes have similar behavior to holes/electrons in semiconductors under a temperature gradient, the differences between i-OTEs and e-OTEs are essential factors to consider when choosing a suitable system for applications. In addition to the significant difference in thermopowers, the overall voltage output response to temperature behaves differently, which will be discussed in the next section. When selecting between eTEs and iTEs, one should consider not only the maximum voltage output that a device can reach but also the output stability. The application scenarios as mentioned above can be representative examples: for a power generator that requires a stable output, an e-OTE system will be a better choice; in contrast, an iTE system can be applied in a real-time, high-sensitivity temperature monitoring device. Although the voltage output of an i-OTE will decay with time, it can reach the maximums rapidly and show the response with a slight temperature change.

3. i-OTE Materials

The basic structure of an ionic thermoelectric device is an ionic electrolyte sandwiched by electrodes. Polymers, ionic liquids, dissociated compounds or their mixtures are the most common materials that serve as electrolytes in an i-OTE system. Among them, polymers can not only function as ion providers but also matrices or gelators. Some polymers have intrinsic mobile ions, which can be driven by a temperature gradient, thus producing an electrical potential between electrodes. Additionally, polymers can serve as matrices (gelators) for ionic liquid, and those 'ionogels' would be more stable and controllable. As for electrodes, conductive materials with a large surface area are preferred, leading to the higher capacitance and power density of the device. In this section, the recently reported materials for i-OTE will be presented and discussed in detail.

3.1. Electrolytes

3.1.1. Polymers

Polymers based on poly(3,4-ethylene-dioxythiophene) (PEDOT) are mixed electronic/ionic conductors, as first reported by Crispin et al. in 2015.[17] These polymers conduct both holes and ions, and their peculiar behaviors can be investigated by adjusting relative humidity (RH) or monitoring the time dependence of open-circuit voltage (V_{OC}). Generally, the presence of water will promote the dissociation of ions, and a higher RH may allow water to form more percolated pathways for ions.[4] Thus, the thermopowers and ionic conductivities of iTE materials will significantly increase with the rising RH, whereas those of an eTE material are barely affected by varying RH in a short period. For PEDOT-based materials, ionic-electronic mixed conducting polymers showed humidity-sensitive characteristics (**Figure 2**a,b).[17] The time dependences of V_{OC} of three types of conductors–pure electronic conductor poly(3,4-dioxythiophene) toluene sulfonate (PEDOT:Tos), pure ionic conductor polystyrene sulfonate (PSS), and mixed electron-ion conductor poly(3,4-ethylenedioxythiophene) polystyrene sulfonate (PEDOT:PSS) are shown in Figure 2c. A pure electronic conductor exhibits a saturated output voltage with a constant ΔT. For an ionic conductor, V_{OC} gradually reaches a high voltage after a long period. For a mixed conductor, V_{OC} increases steadily as ΔT is increasing, reaching a maximum value before ΔT is stabilized. Subsequently, V_{OC} begins to decrease, arrives at a peak, and finally settles to a small value. As shown in Figure 2d, the concentration of holes is increased on the cold side with a temperature gradient applied, resulting in a small value of V_{OC} in the region (i). Then protons diffuse to the cold end, creating an internal electric field, which leads to an opposite cation drift current toward the hot side.

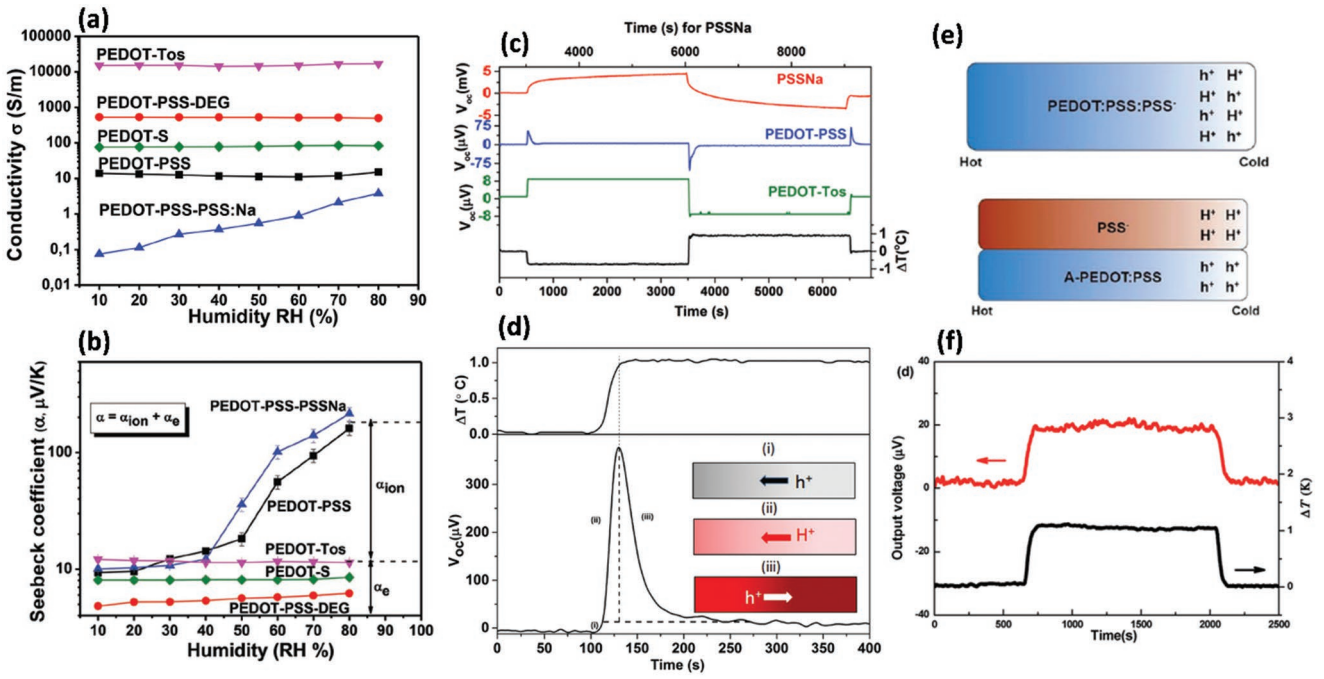

Figure 2. a) Electrical conductivities and b) thermopowers for PEDOT-Tos, PEDOT-PSS-DEG, PEDOT-S, PEDOT-PSS, and PEDOT-PSS-PSS:Na at different humidity. Reproduced with permission.[17] Copyright 2015, Wiley-VCH. c) Open-circuit voltage (V_{OC}) versus time for PEDOT-Tos, PEDOT-PSS, and PSSNa, at 80% RH with $\Delta T = 1$ °C. d) Different regions of the V_{OC}–time curve under a ΔT and the corresponding mechanism. Reproduced with permission.[18] Copyright 2016, Wiley-VCH. e) Schematic cation and hole accumulations under a temperature gradient of PEDOT:PSS:PSSH and PSSH/A-PEDOT:PSS. f) The output voltage measurement across an external load, at 100% RH with a ΔT of 1 °C. Reproduced with permission.[30] Copyright 2018, Royal Society of Chemistry.

The diffusion of protons is reflected in the high value of V_{OC} in the region (ii), and the opposite hole current limits the Soret effect of protons and eventually leads to the decline of V_{OC} in the region (iii). The final constant low voltage is attributed to the neat electronic thermoelectric effect.[18]

In contrast, polyelectrolytes based on polystyrene sulfonate (PSS^-), such as polystyrene sulfonic acid (PSSH) and poly(sodium-4-styrene sulfonate) (PSSNa), are pure ionic conductors, which have impressively high α comparable to those of ionic liquid reported by Yu and Crispin et al.[4,12] The properties of PSSH was measured in both in-plane and out-of-plane directions and matched with each other, confirming the isotropic characteristics of the PSSH film.[4] PSSNa showed α of 4 mV K^{-1}, σ_i of 1.18 S cm^{-1}, and λ of 0.49 W m^{-1} K^{-1}, leading to a zT_i value of 0.012 at 100% RH.[12] The Ouyang group combined these pure ionic conductors into a mixed conductor PEDOT:PSS as a bilayer structure to enhance the thermopower.[30] As shown in Figure 2e, protons in PEDOT:PSS and PSSH layers are present separately in different layers. The accumulated protons in the PSSH layer will generate potential barriers that filter out holes with low energy. Since thermopower is proportional to the difference between the mean energy of transporting charge carriers and the Fermi energy, filtering out the low-energy carriers can increase the mean energy and thus enhance thermopower. The PSSH layer increased thermopower of H_2SO_4-treated PEDOT:PSS from 18.9 to 28.3 μV K^{-1} at an RH of 20%, and was further raised to 43.5 μV K^{-1} at 100% RH. Similar to PSSH, the PSSNa layer can increase thermopower of PEDOT:PSS to 42.5 μV K^{-1} at 100% RH. However, as shown in Figure 2f, the PSSH/PEDOT:PSS exhibits a steady V_{OC}, suggesting that the output voltages arise from the Seebeck effect of holes instead of ions in this bilayer structure.

In addition to the above-mentioned PSSNa and PSSH, various polymers can serve as polyelectrolytes. As shown in **Figure 3**a, Crispin and coworkers reported a device with polyethylene glycol (PEO)-NaOH electrolytes.[26] Adding NaOH to a PEO solution transformed the terminating alcohol groups (—C—OH) into anionic alkoxide end-groups (—C—O—Na^+), and those polycations can be the carriers in the system. The α of PEO-NaOH reached an extremely high value of 11.1 mV K^{-1}, which is 10× higher than eTE materials. Similarly, based on PEO-NaOH, Hu et al. fabricated a cellulosic membrane with natural wood, which naturally aligned cellulose nanofibers and facilitated the transport of Na^+ ions.[31] An aligned cellulosic membrane infiltrated with polymer electrolyte (i.e., PEO-NaOH water solution) exhibited an enhanced α of 19 mV K^{-1}, while the pure polymer electrolyte and polymer-electrolyte-infiltrated randomized cellulosic membrane had α values of only ≈10 and 12 mV K^{-1}, respectively. The electrostatic field surrounding the cellulose nanofibers offered a disparity between the concentrations of cations (Na^+) and anions (OH^-), which aided in the transport of cations and impeded the movement of anions. As a result, the use of an oxidized cellulosic membrane with a higher charge density that provide stronger electrostatic field can further increase α up to 24 mV K^{-1}.

Yu and coworkers compared several polymers, including sulfonated tetrafluoroethylene-based fluoropolymer-copolymer (i.e., Nafion) and sulfonated polyether ether ketone (i.e., S-PEEK)

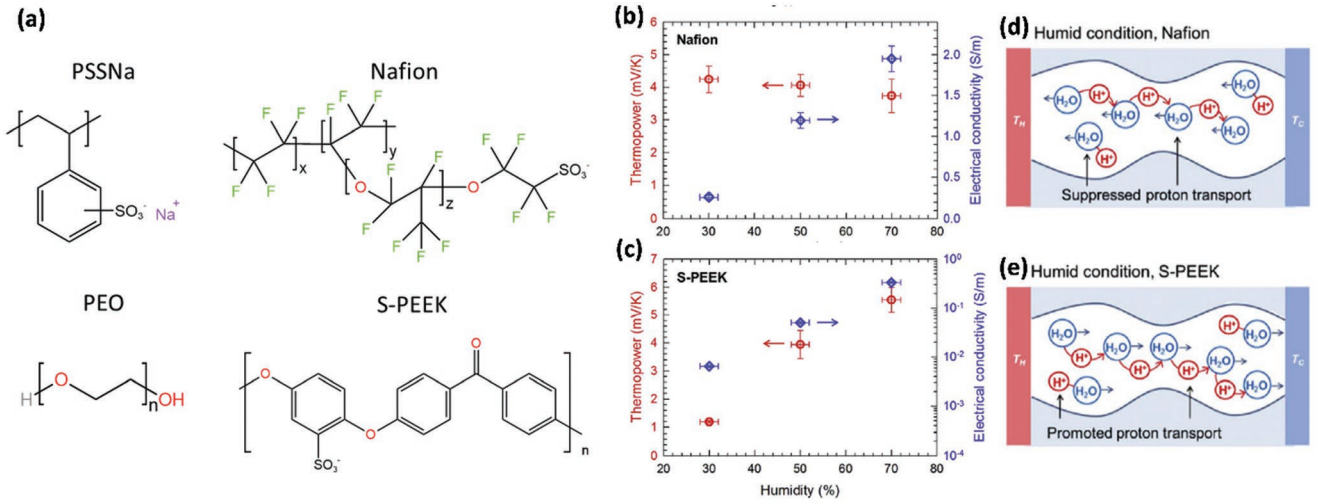

Figure 3. a) Chemical structures of PSSNa, PEO, Nafion and S-PEEK. Thermopower and electrical conductivity of b) Nafion and c) S-PEEK as a function of RH. d) When Nafion is under a humid condition, a thermo-diffusion of the water occurs from the cold side to the hot side, suppressing the proton transport through the water channels. e) When S-PEEK is under a humid condition, the identical thermo-diffusion direction of the water and proton makes the thermoelectric voltage larger with higher humidity. (b–e) Reproduced with permission.[32] Copyright 2018, Elsevier.

with mobile protons.[32] As shown in Figures 3b,c, regarding proton conductors such as Nafion and S-PEEK, as the water content increases, the more percolated pores promote proton hopping and H_3O^+ diffusion, thus increasing σ_i. However, their thermopower behavior appears to be different from each other. In Nafion, the thermo-diffusion direction of the water is opposite to that of the proton (from the hot to cold side), and the proton transport could be impeded by a higher RH (Figure 3d). On the contrary, the proton transport is promoted by the thermo-diffusion of water in S-PEEK, resulting in increasing α with the RH (Figure 3e). The opposite direction of water diffusion results from the hydrophilic properties. Nafion becomes less hydrophilic with increasing temperature, meaning that the hotter side is less stable due to higher entropy. Therefore, water transport in Nafion would occur from the cold to the hot side. S-PEEK becomes more hydrophilic with increasing temperature; hence, the water transport under a temperature gradient would occur from the hot to the cold side. With the high humidity condition of 70% RH, the α of Nafion and S-PEEK were obtained as ≈3.3 and ≈5.5 mV K^{-1}, respectively.

Recently, a ternary polymer polyaniline:poly(2-acrylamido-2-methyl-1-propane sulfonic acid):phytic acid (PANI:PAAMPSA:PA), which is impressively flexible and self-healable, was reported by Jang et al.[27,33] Among it, PAAMPSA provided pathways for proton conduction, offering ionic thermoelectric properties evolved from the Soret effect, while PA acted as a physical crosslinker, interlinking PAAMPSA and PANI via hydrogen bonding. In addition, both PAAMPSA and PA were electrostatically interacted with positively charged PANI. The α reached 8.1 mV K^{-1}, and the σ_i and λ were determined to be 0.237 S cm^{-1} and 0.451 W m^{-1} K^{-1} respectively, which led to a decent zT_i value of 1.04. These properties were well-preserved throughout the test of stretching and self-healing from physically disconnecting, showing the outstanding flexible and self-healable properties of this ternary system. It is worth noting that the binary systems of any combination of these three materials did not have such a self-healing ability since this feature cannot be achieved without multivalent PA or electrostatic interactions between PANI and others.

3.1.2. Ionic Liquid and Hybrids

The abundant and highly mobile ions in ionic liquids (ILs) provide an intrinsic higher α than polymers can produce. Nevertheless, bulky packaging is typically necessary for liquid electrolytes to prevent leakages, which is quite inconvenient for wearable or portable devices. Most reported IL-based materials are made into a quasi-solid 'ionogel' form, adding polymer or oxide particles as gelators. These ionogels afford the advantages of good stability, no leakage concern, and flexibility. For example, Ouyang and coworkers constructed IL/polymer heterostructures and three ILs with different anions, that is, 1-ethyl-3-methylimidazolium tetrafluoroborate (EMIM-BF_4), 1-ethyl-3-methylimidazolium bis(trifluoromethylsulfonyl) imide (EMIM-TFSI) and 1-ethyl-3-methylimidazolium dicyanamide (EMIM-DCA). As an ion donor in IL/polymer hybrid materials, EMIM-DCA showed the best iTE performance among those three ILs when mixed with PEDOT:PSS and PVDF:HFP. The σ_i values of ionogels are consistent with the viscosity of the ionic liquids. EMIM:DCA has the lowest viscosity whose ionogel exhibits the highest σ_i. The highest α from EMIM-DCA/PVDF:HFP ionogel reached 26.1 mV K^{-1}, whose σ_i and λ were 6.7 mS cm^{-1} and 0.176 W m^{-1} K^{-1}, respectively, displaying the typical behavior of an iTE material.[14] In contrast, IL/PEDOT:PSS behaved as an eTE material with relatively low thermopower and high electrical conductivity, both of which are insensitive to the RH level. The time dependence behavior of its V_{OC} also suggested that the IL/PEDOT:PSS heterostructures act like electronic conductors.[34,35] Three imidazolium-based cations with different alkyl chains, RMIM, where R is an ethyl (E), hexyl (H), or decyl (D) group, combined with chloride anions, were compared by Horike and coworkers.[21] With PVA

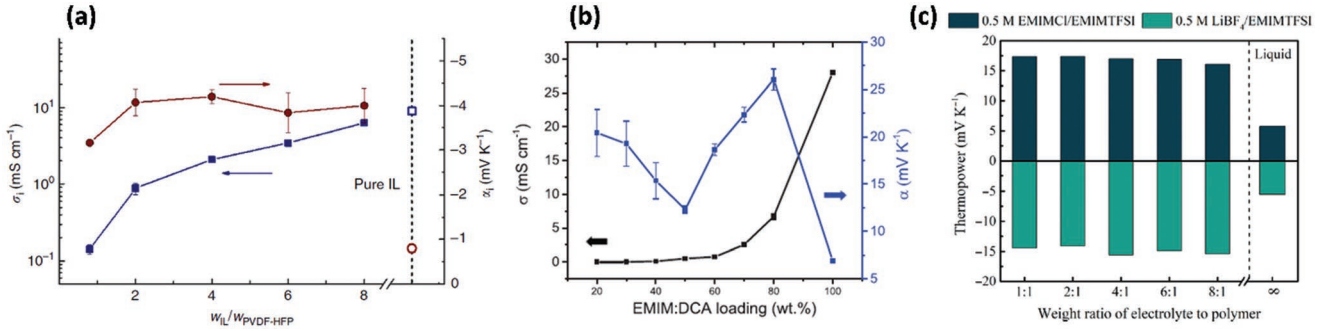

Figure 4. a) Ionic conductivities and thermopowers of EMIM-TFSI/PVDF:HFP ionogel for different weight ratio of liquid electrolyte to polymer matrix. Reproduced with permission.[22] Copyright 2019, Nature Portfolio. b) Ionic conductivities and thermopowers of EMIM-DCA/PVDF:HFP ionogel for different IL loading. Reproduced with permission.[14] Copyright 2019, Wiley-VCH. c) Thermopowers of the p- and n-type EMIM-TFSI/PVDF:HFP ionogels for different weight ratios of liquid electrolyte to polymer matrix. The salt concentration is maintained at 0.5 M. Reproduced with permission.[29] Copyright 2022, American Association for the Advancement of Science.

as a gelator, the gel samples based on EMIM-Cl, HMIM-Cl, and DMIM-Cl have σ_i values of 1.6, 0.75, and 0.63 mS cm^{-1}, respectively. The α values showed a similar tendency with varying alkyl chains of ILs. The α values were determined to be 10.1, 7.2, and 5.9 mV K^{-1} for EMIM-Cl/PVA, HMIM-Cl/PVA, and DMIM-Cl/PVA, respectively. These performance differences can be attributed to the ion mobilities related to molecular sizes.

Generally, higher ILs loading in an IL/polymer system would enhance both α and σ_i due to the increasing carrier concentration (**Figure 4**a).[22,28,36,37] In some cases, the α of binary ionogels has a more complicated behavior with IL loading varying. For instance, the α of EMIM-DCA/PVDF:HFP ionogel exhibited a V-shape dependence on the IL loading, which reached a minimum of 12.3 mV K^{-1} and a maximum of 26.1 mV K^{-1} at the IL loading of 50 and 80 wt.%, respectively (Figure 4b).[14] An ionogel of EMIM-TFSI/PVDF:HFP doped with $LiBF_4$ or EMIM-Cl had the α almost independent of the electrolyte/polymer weight ratio (Figure 4c).[29] It is worth noticing that polymers not only serve as matrices or gelators, but also the interactions between polymers and ionic liquid can enhance the overall thermoelectric performance in most IL/polymer systems. More recently, Ouyang et al. reported a α value of 26.1 mV K^{-1} for EMIM-DCA/PVDF:HFP ionogel, which is much higher than that (6.9 mV K^{-1}) of neat EMIM-DCA.[14] Similar phenomena were also observed by Huang and coworkers in EMIM-TFSI/PVDF:HFP systems. With only ≈10 wt.% PVDF:HFP content, the α of the ionogel was dramatically enhanced from 5.8 to ≈15 mV K^{-1}.[29] The significant enhancements of α can be ascribed to the ionic thermo-diffusion boosted by the interaction between ions and the PVDF:HFP. When forming a binary gel with ILs, the PVDF:HFP had a phase transformation from α-phase to highly polar β-phase with CH_2 dipoles positively charged and CF_2 negatively charged. The dipoles interact with cations and anions, increasing the heat of transport (Q^*) without obvious selectivity. Therefore, the mobility difference between cations and anions is enlarged, leading to a higher α.[28,29]

3.2. Additives

The primary function of additives for electrolytes can be summarized into two types–providing ions and raising the mobility difference between cations and anions. An acidic or basic can function as an ion supplier, increasing the carrier concentration and thus enhancing the α.[32] On the other hand, polymers or particles acting as Lewis acid or base can selectively interact with one type of ions in an electrolyte, which adjusts the difference in mobility between cations and anions, and thus improve or reverse the sign of α.[13]

3.2.1. p-Type Enhancement/Transition

Yu et al. investigated the effect of H_3PO_4 and NaOH on polyvinyl alcohol (PVA).[32] With the H_3PO_4 as cation supplier, the PVA-H_3PO_4 produced a positive α of 1.6 mV K^{-1} which was maintained over a wide range of RH levels. Since the Soret coefficient of H^+ in H_3PO_4 is much larger than anions in the system, which indicate the stronger diffusion of cations from the hot to the cold side, the ionogel performed as p-type iTE material with positive α. According to a recent report by Ouyang and coworkers, SiO_2 nanoparticles featured Lewis acidic hydroxy groups on the surface, which would strongly attract anions of EMIM-DCA.[13] In this regard, the mobility difference between cations and anions was enlarged, and accessible volume for ion transport was created since the short-range ordering was disrupted. As a result, both α and σ_i that are dependent on ion mobility would be enhanced. Furthermore, SiO_2 nanoparticles can function as a gelator similar to a polymer matrix. The C≡N group of EMIM-DCA interacts with polar −OH groups on the surface of SiO_2 nanoparticles, forming solid networks and making the EMIM-DCA/SiO_2 behave as an ionogel. An optimal zT_i value of the ionogel reached 1.47 with the addition of SiO_2 nanoparticles at room temperature, among which α was 14.8 mV K^{-1}, and σ_i and λ were 47.5 mS cm^{-1} and 0.21 W m^{-1} K^{-1}, respectively.

By contrast, polyethylene glycol (PEG) can play the role of Lewis base in electrolytes and preferentially interact with cations.[22] The α and σ_i with various concentration ratios C_{PEG}/C_{IL} are shown in **Figure 5**a. In an EMIM-TFSI/PVDF:HFP ionogel, PEG formed hydrogen bonds with EMIM, which disturbed the cation-anion pairs of the IL and thus promoted ionic dissociation. An initial increase in σ_i originated from the enhancement in the degree of dissociation and

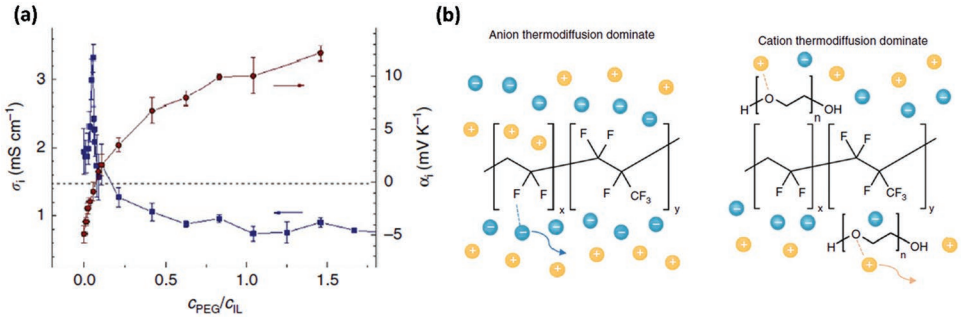

Figure 5. a) Ionic conductivities and thermopowers of the EMIM-TFSI/PVDF:HFP gels at different PEG contents. b) Schematic illustration of the change in thermopower of the polymer gels. Reproduced with permission.[22] Copyright 2019, Nature Portfolio.

carrier mobility. A sequential drop of σ_i at C_{PEG}/C_{IL} of 0.052 could be attributed to the decreasing ion mobility due to the increased viscosity with higher PEG concentration. Finally, σ_i reached a plateau for $C_{PEG}/C_{IL} > 0.21$, with the degree of dissociation and carrier mobility remaining constant. Figure 5b illustrates the mechanism of thermal diffusion with and without the presence of PEG in the IL/polymer system. In the absence of PEG, PVDF promoted the thermal diffusion of $TFSI^-$ anions over cations as a temperature gradient was applied, resulting in a negative α. After PEG was induced, the interaction between PVDF and anions was disrupted by PEG chains, and the oxygen atoms of PEG interacted with cations, promoting the thermal diffusion of $EMIM^+$ cations. Hence, the overall α of PEG/EMIM-TFSI/PVDF:HFP shifted toward positive with increasing C_{PEG}/C_{IL}, which switched to a p-type material with positive α for $C_{PEG}/C_{IL} > 0.052$, achieving a desired p-n conversion for i-OTE ionogel. Similarly, a conversion from n- to p-type in EMIM-TFSI/PVDF:HFP was also reported in recent work of Huang et al.[29] Adding EMIM-Cl provided additional Cl^- ions that formed hydrogen bonds with cations ($EMIM^+$), which increased the Q^* of cations and led to a cation-dominant electrolyte based on EMIM-TFSI/PVDF:HFP with positive α.

3.2.2. n-Type Enhancement

As mentioned in previous section, Yu et al. reported an α of PVA-NaOH was ≈–1 mV K^{-1} and similarly insensitive to humidity. The negative α can be attributed to the higher Soret coefficient of OH^- in the system, which is analogous to the positive α produced by PVA-H_3PO_4 electrolyte.[32] The Huang group reported a significant n-type α improvement of EMIM-TFSI/PVDF:HFP ionogel upon the addition of $LiBF_4$, which increased from –4 to a maximum value of –15 mV K^{-1}.[29] The additional Li^+ ions established a strong interaction with anions ($TFSI^-$ and BF_4^-) in electrolyte and enlarged the Q^* of anions, leading to higher negative α.

In contrast to the additives that can realize p- to n-type transition mentioned above, however, there is no known additive that can converse p-type electrolyte to n-type one. Although there is report that adjusting water content in electrolyte can modify EMIM-Ac from p- to n-type, which will be discussed later in Section 4.2, the methods that can produce n-type i-OTEs paired with p-type counterpart remain scarce. The electrical transport performance of recently reported i-OTE electrolytes is summarized in **Table 2**.

3.3. Electrodes

For an ITESC, a suitable electrode material is crucial to achieve better capacitance and energy density and further improve the performance of the device in practical applications. Both Au and Ag electrodes are mostly used since they have excellent electrical conductivity and electrochemical stability;[12,14,21,27,38] graphite[39] or carbon nanotubes (CNTs)[14,27] and their composites with gold or silver[13,26] are also common choices since their large surface area can lead to a higher capacitance of devices. In addition, polymers were investigated to be applied in devices as electrodes in recent years,[25] which afford more prospects to reach a better supercapacitor performance.

As shown in **Figure 6**a, the cyclic voltammetry (CV) curves of EMIM-DCA-based ionic thermoelectric capacitors with single-walled carbon nanotubes (SWCNTs) or Ag as electrodes indicated that SWCNTs could give rise to higher capacitance than Ag. The total energy delivered by the ITESC also dramatically increased from 3360 to 12 300 μJ m^{-2} with the Ag electrodes replaced by SWCNT electrodes. The improvement can be ascribed to the higher specific surface area of SWCNT electrodes. Moreover, the shape of voltage profiles of forward and reverse electronic working (stages ii and iv, as mentioned in Section 2.3) are not exactly the same, which might result from the ion-electron attraction at the electrode in stage ii (Figure 6b,c).[14] It follows that the interaction between electrolytes and electrodes should be considered when choosing the electrode materials. Horike et al. reported that EMIM-Cl-based ITESCs with different transition metals serving as electrodes had distinct behavior of voltage response to the temperature gradient.[21] Figure 6d,e shows the behavior of V_{OC} of two typical types in response to the temperature difference. A stable voltage could be obtained using Ag or Pt electrodes, while a transient behavior of V_{OC}, which immediately decays after reaching the extreme, was observed when using Au or Ni electrodes. The difference is a combined result of the Soret effect and the interaction between ions and metal electrodes. A thermopower from the metal/electrolyte contribution resulted from the thermal-induced polarization at the interface of electrolyte and electrodes (Figure 6f), which is dependent on the effective surface ion charge and the electric double-layer capacitance. Experiments further proved that temperature-dependent capacitance was one of the main contributors to the output voltage of ionic hydrogels when measured with Ag electrodes. On the other hand, the ion diffusion

Table 2. A summary of thermopowers and ionic conductivities of recently reported electrolytes.

Electrolyte	RH	Thermovoltage [mV K^{-1}]	Ionic Conductivity [S cm^{-1}]	Reference
PSSNa	100%	4	1.18	[12]
PSSH	70%	7.9	9	[4]
PEO-NaOH		11.1	8.13×10^{-5}	[26]
PEO-NaOH		7		[38]
Nafion	70%	≈3.3	≈1.9	[32]
S-PEEK	70%	≈5.5	≈0.2	
PVA-NaOH	70%	−1	≈0.6	
PVA-H_3PO_4	70%	1.6	≈2.9	
PANI:PAAMPSA:PA	50%	8.1		[33]
PANI:PAAMPSA:PA/SiO_2	80%	17.9	0.187	[27]
PSSH/graphene oxide		≈12.6	0.114	[40]
NaOH/PEO/water (infiltrated oxidized cellulosic membrane)		24	≈0.1	[31]
EMIM-Ac/water		2.413		[44]
EMIM-Ac/water		−0.918		
EMIM-Cl/PVA		10.1	1.6×10^{-3}	[21]
EMIM-DCA/SiO_2		14.8	4.75×10^{-2}	[13]
EMIM-DCA/PVDF:HFP		26.1	6.7×10^{-3}	[14]
EMIM-DCA/PVDF:HFP	70–75%	25.4	1.76×10^{-2}	[36]
EMIM-DCA/PVDF:HFP/Na-DCA	85%	43.8	1.94×10^{-2}	[42]
EMIM-DCA/BC		18.04	2.88×10^{-2}	[45]
EMIM-OAC/PEO/P123	60%	1.8	1.1×10^{-3}	[37]
EMIM-TFSI/PVDF:HFP		−4	2×10^{-3}	[22]
EMIM-TFSI/PVDF:HFP/PEG		14	8×10^{-4}	
EMIM-TFSI/PVDF:HFP		−3.8	2.34×10^{-3}	[25]
EMIM-TFSI/PVDF:HFP/$LiBF_4$		−15	4.5×10^{-3}	[29]
EMIM-TFSI/PVDF:HFP/EMIM-Cl		17	4×10^{-3}	
Na-TFSI/PVDF:HFP/PC	68%	20	2.6×10^{-3}	[28]
Na-TFSI/PVDF:HFP/PC/TPFPB	68%	≈−5	1.5×10^{-3}	
I^-/I_3^- /MC/KCl		−8.18	3.6×10^{-2}	[39]
		9.62	3.6×10^{-2}	
ChCl:EG/WPU	90%	19.5	8.4×10^{-3}	[46]
EMIM-OTf/PVDF:HFP	90%	38.3	1.1×10^{-2}	[47]

based on the Soret effect was the main contributor to the output voltage of ionic hydrogels with Au electrodes. Consequently, the voltage response could vary with different metals used as electrodes, which depend on the ion-metal interaction on the interface.

As discussed previously, PEDOT:PSS is an ion/electron mixed conductor, which can be utilized as the electrodes of ITESCs. Crispin and coworkers proved that the interface between PEDOT:PSS electrodes and the EMIM-TFSI/PVDF electrolyte was stable, and ions of the ionogel can penetrate the PEDOT:PSS layer.[25] They also found that the thermo-induced voltage was markedly enhanced with increasing PSS content in electrodes. Accordingly, the device with PSS/Au electrodes (PSS content of 100%) showed the highest α, while that with PEDOT-Tos (PSS content of 0%) exhibited the lowest (**Figure 7**a). As shown in Figure 7b, this result can be explained by the PSS-induced Donnan-like potential, which can significantly affect the thermo-voltage in the ITESCs with PEDOT electrodes.

4. Performance Optimization of i-OTEs

4.1. Power Factor

As noted in Section 2.1, the performance of iTE materials can be stated by the dimensionless ionic figure of merit zT_i, which is dependent on the absolute temperature, the electrical transport properties (i.e., power factor, PF = $\alpha\sigma_i$) and the thermal conductance (i.e., total thermal conductivity, λ) of the materials. Increasing PFs of materials is the main target for zT_i value enhancement since organic materials generally have intrinsic low λ.

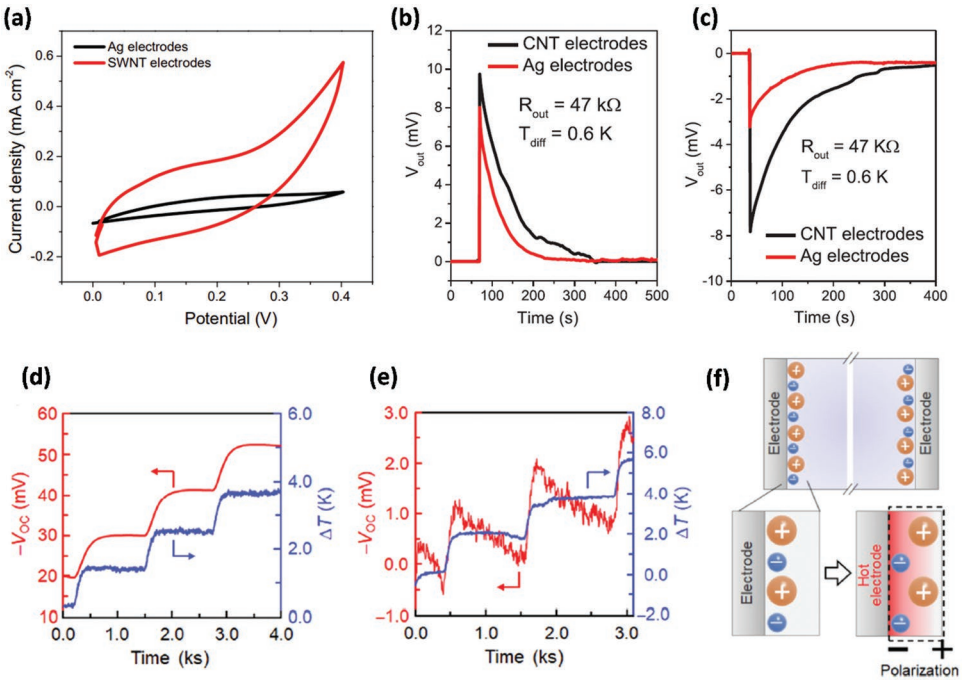

Figure 6. a) Cyclic voltammograms of EMIM-DCA-based ITESCs with Ag or SWCNT as the electrodes. b) Forward electronic working and c) reverse electronic working using Ag or SWCNT electrodes. Reproduced with permission.[14] Copyright 2017, Wiley-VCH. Temporary change of open circuit voltage from Emim-Cl/PVA hydrogel measured by d) Ag paste and e) Au electrodes with the supplied temperature differences. f) Schematic of possible mechanism of open-circuit voltage (V_{OC}) generation under temperature gradient by the contribution of metal-electrolyte interface. Reproduced with permission.[21] Copyright 2020, American Chemical Society.

In addition to common methods such as adjusting IL loading, adding ion suppliers or additives that can selectively facilitate ion mobility described in Section 3, some novel methods that have been proven effective for PF enhancement will be stated in this section. It should be noted that, unlike conventional eTE materials, the α and the σ_i of an iTE material are positively correlated with ion mobility so that they usually can be improved simultaneously without compromise.[12,17,40,41] The humidity condition of the environment or the water content can considerably affect the power factor of polymeric iTE materials,[4,12,17,18,32,33,42,43] which is distinct from eTE materials. Yu et al. reported the enhancement of σ_i and α of a PSSH/graphene oxide hydrogel from ≈7.5 S m^{-1}/8.4 mV K^{-1} to ≈11.4 S m^{-1}/12.6 mV K^{-1} as the water uptake was increased from 10 to 40 wt.%, respectively.[40] Crispin and coworkers recently showed that the α of PSSNa can be significantly increased from 0.26 mV K^{-1} at 50% RH to 4 mV K^{-1} at 100% RH while σ_i was enhanced from 0.026 to 1.18 S m^{-1}, accordingly.[12] The ternary polymeric material PANI:PAAMPSA:PA reported by Jang et al. exhibited an increase of σ_i and α from 0.0139 S m^{-1}/1.3 mV K^{-1} at 50% RH to 0.256 S m^{-1}/8.1 mV K^{-1} at 90% RH.[33] The enhancement of thermopowers and ionic conductivities can be ascribed to multiple effects of water in i-OTE systems with various materials. According to Yu and coworkers' report, in a PSSH/graphene oxide electrolyte, the presence of water molecules can facilitate ion diffusion and thus increase ionic conductivities. Since the thermo-diffusion directions of water molecules coincide with protons, the thermo-induced protons diffusion was hard to revert, which yielded a higher ionic thermopower.[40] On the other hand, with an increasing humidity, the absorbed water

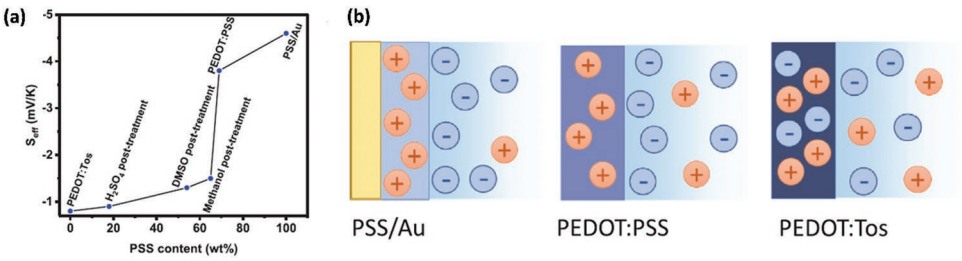

Figure 7. a) The thermo-induced voltage coefficients of devices composed of different electrodes with various PSS contents. b) Illustration of the charge distribution at the electrode/electrolyte interface. Reproduced with permission.[25] Copyright 2021, Wiley-VCH.

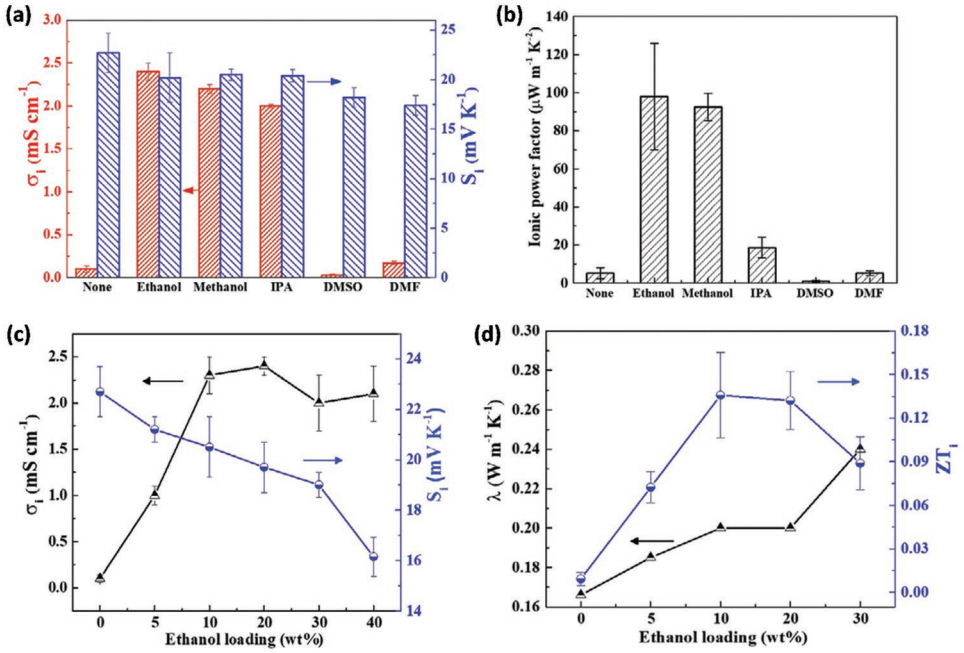

Figure 8. a) Ionic conductivities and ionic thermopowers and b) ionic power factors of PVDF:HFP/EMIM-DCA-50% ionogels prepared from solutions added with different antisolvents prior to the ionogel formation. c) The ionic conductivities and ionic thermopowers and d) thermal conductivities and zT_i value of the PVDF:HFP/EMIM-DCA ionogels on the ethanol loading in solution. Reproduced with permission.[36] Copyright 2021, Wiley-VCH.

molecules in the hygroscopic polyelectrolyte formed a solvation shell. Consequently, the electrostatic attraction between the mobile ions and immobile polyions is suppressed, which decreases the activation energy for transporting mobile ions.[12] Furthermore, the increase in humidity leads to more water percolation paths, i.e., conduction channels in the polyelectrolyte. Although the λ was slightly increased due to the more percolation pathways that were thus created, the zT_i had an impressive increase of four orders of magnitude.[4]

Most reported polymeric and IL/polymer electrolytes have satisfying performance at the high humidity level of 70–100% RH. However, such a high humidity is not suitable for practical application because the optimum humidity for human health and comfort is 40–60%.[37] In that case, it might be inappropriate to excessively increase the humidity of the environment and reach the best performance of iTE materials. As mentioned above, the competitive performance of 1-ethyl-3-methylimidazolium acetate (EMIM-OAC)/PEO/(polyethylene oxide-polypropylene oxide-polyethylene oxide (P123) ternary material at a relatively low humidity reported by Jiang et al. offered a viable route to develop more favorable materials for applications.[37]

Ouyang and coworkers recently showed that adding antisolvent during the solution preparation process can effectively change the solid networks and thus enhance the σ_i of the subsequently formed ionogel.[36,42] As shown in **Figure 8**a, the σ_i of the EMIM-DCA/PVDF:HFP ionogel was significantly increased with the addition of antisolvent ethanol, methanol, or isopropyl alcohol (IPA), among which ethanol was the most effective antisolvent to enhance the PF (Figure 8b). The effect of the antisolvent addition on the σ_i of the EMIM-DCA/PVDF:HFP ionogels can be explained by the solvent effect on the solid networks of the PVDF:HFP chains. The reduced grain size of the ionogel networks with antisolvent addition resulted in more grain boundaries, facilitating ion transport and increasing the σ_i. Despite the minor decrease in α and increase in λ, the zT_i values were noticeably enhanced with the ethanol loading of 10 wt.% (Figure 8c,d), showing that adding antisolvent is an effective way to improve the overall performance of a PVDF:HFP-based ionogel. However, it should be noted that the antisolvent pretreatment has not been applied on ionogels with other polymer matrices but PVDF:HFP. Therefore, the effect on different polymers needs further investigation for broader use.

4.2. P-N Conversion

Although iTE materials have impressively high thermopower compared with eTE materials, it is inevitable that constructing a structure with p-, n-type legs connected electrically in series and thermally in parallel (Figure 1a) will be required for further large-scale applications. In this respect, finding suitable p- and n-type materials is indispensable for iTE materials development. A valid method is to modify the type of mobile ions in an electrolyte,[22,28,29] so that p-n pairs based on the same material can fit in the same application environment. However, most iTE materials are p-type since cations are usually more mobile than anions in electrolytes, as the reported i-OTEs shown in **Figure 9**, meaning the scarcity of n-type iTE materials is an urgent problem to be solved.

Adding compounds or polymers is one most common method to realize the p-n conversion of i-OTEs,[22,28,29] which was discussed in Section 3.2. Additionally, modifying the water content or the environment temperature can effectively achieve p-n conversion for specific electrolytes. Wang and coworkers

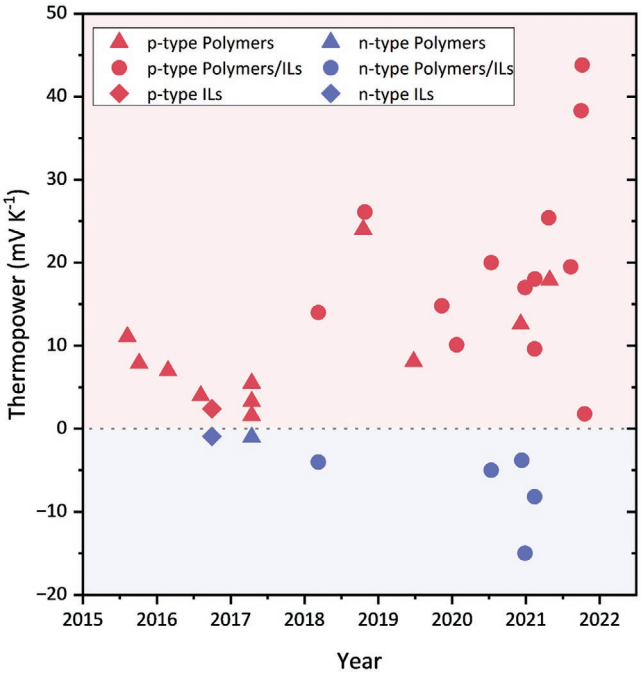

Figure 9. Evolutional progress of the thermopower improvements in i-OTEs.

reported a p-n conversion of a water/EMIM-Ac binary liquid system with precise control over water content.[44] They found a watershed of p-n conversion between the water content of 30 and 35 wt.% in the water/EMIM-Ac system (**Figure 10**a), which can be attributed to the change of cluster species with higher desorption velocity. As shown in Figure 10b,c, with the increased water content, more water molecules grafted onto EMIM-Ac/2W (referred to an EMIM-Ac molecule with two water molecules) cluster, and EMIM-Ac/4W with higher thermodynamic stability was formed. With the molar ratio of water exceeding 4:1 in the binary system, the cations and anions of IL became entirely separated by water molecules (Figure 10d). With anions surrounded by hydration layers, the initially strong interaction between anion clusters and Au turned weaker than the cation-gold interaction (Figure 10e,f). As a result, the anions served as the major charge carriers instead of cations with the water content above 30 wt.% in the electrolyte, leading to a p- to n-type conversion. The highest p-type and n-type α of this water/EMIM-Ac system were determined to be 2.413 ± 0.020 mV K^{-1} at the water content of 15 wt.% and –0.918 ± 0.034 mV K^{-1} at the water content of 35 wt.%, respectively. A module was constructed with five p-n pairs of water/EMIM-Ac, reaching an output voltage of 247.68 ± 1.40 mV with a ΔT of 15 K.

A liquid electrolyte consisting of methylcellulose (MC) and I^-/I_3^- ions which afforded a temperature-induced p-n conversion was reported by Xu et al.[39] The ion polarization switching can be ascribed to the reversed reactions at two electrodes induced by the hydrophobic interaction between I_3^- and MC. As shown in **Figure 11**, MC gradually became hydrophobic at the hot electrode while remaining hydrophilic at the cold electrode. As the temperature of the hot side was increased, MC formed complexes with I_3^- ions through the hydrophobic interaction and resulted in a lower concentration of free I_3^- ions. With the temperature of the hot side reaching the transition temperature (T_{Tra}), the concentration of I_3^- ions was much lower than that of I^- ions, and the reversed reactions will occur at two electrodes. For the two situations of n-type and p-type, the reactions at two electrodes are summarized in **Table 3**. After further optimization with KCl addition, the p-type and n-type α reached 9.62 and –8.18 mV K^{-1}, respectively. Nevertheless, this MC/I/KCl ternary material might be unsuitable to serve as p-n pairs in devices at this point since the p- and n-type behavior would appear in different temperature ranges. Therefore, extra investigation or peculiar device structure designs are still required to compensate for this difficulty.

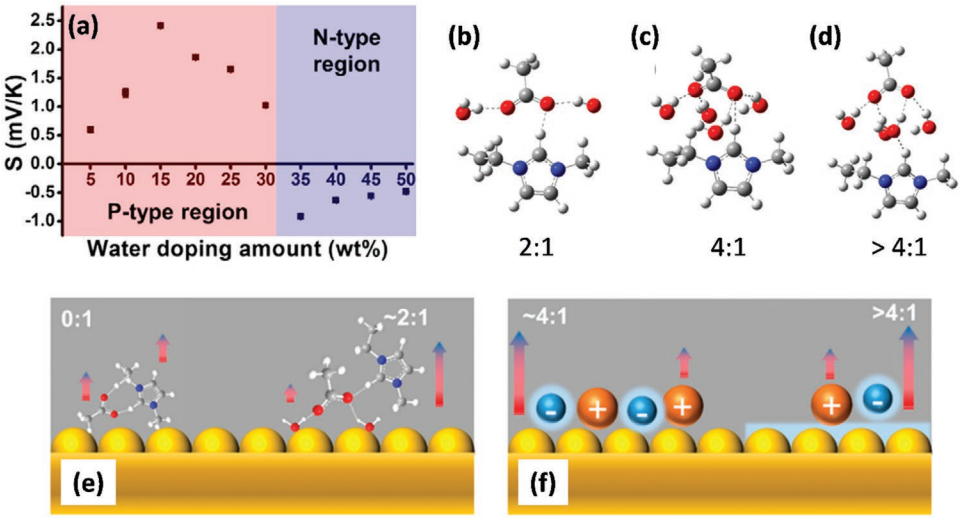

Figure 10. a) Thermopowers of different water/EMIM-Ac binary systems with corresponding mass fraction of water. b–d) Density functional calculated configurations of water/EMIM-Ac clusters in corresponding with molar ratio of 2:1, 4:1 and above. e,f) Schematic illustration of ionic desorption behaviors of water/EMIM-Ac binary systems with different water/IL molar ratios. Hydration layer of water–anion clusters is marked with light blue loop-shaped backgrounds. Reproduced with permission.[44] Copyright 2017, American Chemical Society.

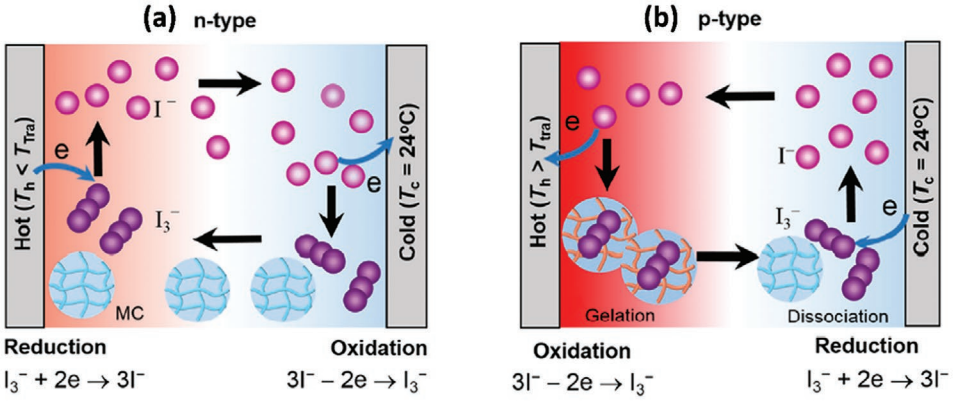

Figure 11. Schematics of the polarization switching from a) n-type ($T_h < T_{Tra}$) to b) p-type ($T_h > T_{Tra}$) induced by the gelation of MC. Reproduced with permission.[39] Copyright 2022, American Association for the Advancement of Science.

5. Conclusions and Outlook

To summarize, by choosing suitable electrolytes and functional additives, the overall performance of i-OTE materials has been significantly improved in recent years. The state-of-the-art thermopower of most i-OTEs has now exceeded 15 mV K^{-1},[13,14,27–29,36,42,45] which is approximately a hundred times larger than conventional e-OTEs. Among the three main types of i-OTEs: polymers, ILs, and their hybrids, the IL/polymer systems generally afford the highest thermopower. Their better stability and controllability resulting from the quasi-solid properties are also more suitable for various application scenarios, which makes IL/polymer systems the most promising candidate for further research thrusts.

However, as a newly developing field, there still exist noticeable weaknesses of iTE materials yet to be solved. One most critical issue of i-OTE materials, for instance, is the much lower σ_i than the σ of e-OTEs, which results in low zT_i values and poor device performances. Although several methods have manifested effective for the σ_i enhancement, the improvement of i-OTEs' overall performance remains limited. In this respect, further studies should pay more attention to the σ_i optimization rather than focusing merely on the thermopower enhancement as most reported works did. Another challenge lies in the scarcity of n-type i-OTE materials. To meet the needs of large-scale applications in the future, the device structure consisting of p-n junctions will be crucial to achieving more efficient production. In spite of adjusting water content and varying hot-side temperature (T_H) mentioned in Section 4.2 are effective methods for p-n alteration, the incidental problems such as liquid leakage might hinder their further applications. Since the intrinsic p-type behavior of most i-OTE materials result from free cations and immobile anions, modifying the main mobile ions with additives that selectively interacting with one type of ions will be an effective and more suitable method to realize p-n conversion. Until now, several i-OTE materials have been modified into p- and n-type and both types maintain the merit of high thermopower, holding good promise for practical applications and providing a viable direction to follow in future works.

Table 3. Possible reactions occurred at two electrodes in MC/I^-/I_3^- electrolyte.

n-type[39]	Hot side:	$I_3^- + 2e \rightarrow 3I^-$
	Cold side:	$3I^- - 2e \rightarrow I_3^-$
p-type	Hot side:	$3I^- - 2e \rightarrow I_3^-$
	Cold side:	$I_3^- + 2e \rightarrow 3I^-$

After decades of deployment, conventional TEG devices have proven to be an effective alternative energy source, capable so far of providing sufficient power for small devices. However, further applications in lightweight, small-sized portable devices will be limited by the large number of p-n units required for power generation. In this context, i-OTEs with intrinsically high thermopower offer a potential option for expanding the application of thermoelectric technologies. The application of i-OTEs in ITESC has been investigated in most research reports, but ITESCs have not yet been utilized in practical scenarios due to the low efficiency that is insufficient for electronic devices. Given that the efficiency of ITESCs depends largely on the zT_i values of materials, the improvement of overall iTE performances of electrolytes will be the prior target before being applied in capacitors. On the other hand, employing i-OTEs as thermal sensors might be more serviceable for the moment. A thermal sensor can take full advantage of the high thermopowers of i-OTEs, and its relatively simple structures are easier to produce and more portable. For instance, sensitive temperature sensing devices for health monitoring or environmental regulation will be useful in daily life, and their light weight, small size, and superior mechanical flexibility will be advantageous for wearable or mobile devices.

Even with some challenges to be resolved, the applications of i-OTEs are still viable and promising since their remarkably high thermopowers offer alternate potential applications. Given that i-OTEs and e-OTEs feature their respective merits of superb thermopower and high electrical conductivities, an integral system combining both types of OTEs seems to be a prospective proposal for highly demanding applications. However, the hurdle of such integration lies in the distinctive applications of i-OTEs and e-OTEs, making their combination challenging to accomplish at the current stage. On the other hand, considering that Liu et al. recently reported an inorganic

ionic thermoelectric/thermogalvanic (TG) synergistic system that combined the thermodiffusion of ions and the TG effect of redox couples,[48] indicating that it might be a viable avenue in future works for i-OTEs to develop hybrid systems with other technologies such as TGs or eTEs. At present, novel i-OTEs with impressive performance are largely under exploration, including some functional materials with better mechanical properties, flexibility, and self-healing abilities. Since the conventional e-OTEs have been investigated for years and almost reach their full development, the burgeoning i-OTEs have shown their great application prospect and may break new ground for organic thermoelectrics.

Acknowledgements

The work was financially supported by National Natural Science Foundation of China (NSFC) under grant No. 61890940 (Y.Z.) and the Science and Technology Commission of Shanghai Municipality (STCSM) under grant No. 21520710900 (Z.L.).

Conflict of Interest

The authors declare no conflict of interest.

Keywords

ionic conductivity, ionic organic thermoelectrics, ionic thermoelectric supercapacitors, Soret effect, thermopower

Received: July 22, 2022
Revised: September 1, 2022
Published online:

[1] J. Mao, G. Chen, Z. Ren, *Nat. Mater.* **2021**, *20*, 454.
[2] S. Xu, X.-L. Shi, M. Dargusch, C. Di, J. Zou, Z.-G. Chen, *Prog. Mater. Sci.* **2021**, *121*, 100840.
[3] Q. Yan, M. G. Kanatzidis, *Nat. Mater.* **2022**, *21*, 503.
[4] S. L. Kim, H. T. Lin, C. Yu, *Adv. Energy Mater.* **2016**, *6*, 1600546.
[5] D. Zhao, A. Würger, X. Crispin, *J Energy Chem* **2021**, *61*, 88.
[6] H. Cheng, Q. Le, Z. Liu, Q. Qian, Y. Zhao, J. Ouyang, *J. Mater. Chem. C* **2022**, *10*, 433.
[7] G. Chen, M. S. Dresselhaus, G. Dresselhaus, J. P. Fleurial, T. Caillat, *Int. Mater. Rev.* **2003**, *48*, 45.
[8] F. J. DiSalvo, *Science* **1999**, *285*, 703.
[9] M. Hamid Elsheikh, D. A. Shnawah, M. F. M. Sabri, S. B. M. Said, M. Haji Hassan, M. B. Ali Bashir, M. Mohamad, *Renew. Sust. Energ. Rev.* **2014**, *30*, 337.
[10] J. Zang, J. Chen, Z. Chen, Y. Li, J. Zhang, T. Song, B. Sun, *J. Mater. Chem. A* **2021**, *9*, 19439.
[11] D. M. Rowe, *CRC handbook of thermoelectrics*, CRC press, Boca Raton, FL, **1995**.
[12] H. Wang, D. Zhao, Z. U. Khan, S. Puzinas, M. P. Jonsson, M. Berggren, X. Crispin, *Adv. Electron. Mater.* **2017**, *3*, 1700013.
[13] X. He, H. Cheng, S. Yue, J. Ouyang, *J. Mater. Chem. A* **2020**, *8*, 10813.
[14] H. Cheng, X. He, Z. Fan, J. Ouyang, *Adv. Energy Mater.* **2019**, *9*, 1901085.
[15] Y. Chen, Y. Zhao, Z. Liang, *Energy Environ. Sci.* **2015**, *8*, 401.
[16] L. Zhang, X.-L. Shi, Y.-L. Yang, Z.-G. Chen, *Mater. Today* **2021**, *46*, 62.
[17] H. Wang, U. Ail, R. Gabrielsson, M. Berggren, X. Crispin, *Adv. Energy Mater.* **2015**, *5*, 1500044.
[18] U. Ail, M. J. Jafari, H. Wang, T. Ederth, M. Berggren, X. Crispin, *Adv. Funct. Mater.* **2016**, *26*, 6288.
[19] M. Bonetti, S. Nakamae, B. T. Huang, T. J. Salez, C. Wiertel-Gasquet, M. Roger, *J. Chem. Phys.* **2015**, *142*, 244708.
[20] S. Masoumi, S. O'Shaughnessy, A. Pakdel, *Nano Energy* **2022**, *92*, 106774.
[21] S. Horike, Q. Wei, K. Kirihara, M. Mukaida, T. Sasaki, Y. Koshiba, T. Fukushima, K. Ishida, *ACS Appl. Mater. Interfaces* **2020**, *12*, 43674.
[22] D. Zhao, A. Martinelli, A. Willfahrt, T. Fischer, D. Bernin, Z. U. Khan, M. Shahi, J. Brill, M. P. Jonsson, S. Fabiano, X. Crispin, *Nat. Commun.* **2019**, *10*, 1093.
[23] Y. Chen, X. Hou, C. Ma, Y. Dou, W. Wu, *Adv. Mater. Sci. Eng.* **2018**, *2018*, 1210562.
[24] Z. Soleimani, S. Zoras, B. Ceranic, S. Shahzad, Y. Cui, *Sustain. Energy Technol. Assess.* **2020**, *37*, 100604.
[25] S. Mardi, D. Zhao, N. Kim, I. Petsagkourakis, K. Tybrandt, A. Reale, X. Crispin, *Adv. Electron. Mater.* **2021**, *7*, 2100506.
[26] D. Zhao, H. Wang, Z. U. Khan, J. C. Chen, R. Gabrielsson, M. P. Jonsson, M. Berggren, X. Crispin, *Energy Environ. Sci.* **2016**, *9*, 1450.
[27] Y. T. Malik, Z. A. Akbar, J. Y. Seo, S. Cho, S.-Y. Jang, J.-W. Jeon, *Adv. Energy Mater.* **2022**, *12*, 2103070.
[28] C. Chi, M. An, X. Qi, Y. Li, R. Zhang, G. Liu, C. Lin, H. Huang, H. Dang, B. Demir, Y. Wang, W. Ma, B. Huang, X. Zhang, *Nat. Commun.* **2022**, *13*, 221.
[29] S. Liu, Y. Yang, H. Huang, J. Zheng, G. Liu, T. H. To, B. Huang, *Sci. Adv.* **2022**, *8*, eabj3019.
[30] X. Guan, H. Cheng, J. Ouyang, *J. Mater. Chem. A* **2018**, *6*, 19347.
[31] T. Li, X. Zhang, S. D. Lacey, R. Mi, X. Zhao, F. Jiang, J. Song, Z. Liu, G. Chen, J. Dai, Y. Yao, S. Das, R. Yang, R. M. Briber, L. Hu, *Nat. Mater.* **2019**, *18*, 608.
[32] S. L. Kim, J.-H. Hsu, C. Yu, *Org. Electron.* **2018**, *54*, 231.
[33] Z. A. Akbar, J.-W. Jeon, S.-Y. Jang, *Energy Environ. Sci.* **2020**, *13*, 2915.
[34] J. Wang, Q. Li, K. Li, X. Sun, Y. Wang, T. Zhuang, J. Yan, H. Wang, *Adv. Mater.* **2022**, *34*, 2109904.
[35] Z. Fan, D. Du, X. Guan, J. Ouyang, *Nano Energy* **2018**, *51*, 481.
[36] Z. Liu, H. Cheng, H. He, J. Li, J. Ouyang, *Adv. Funct. Mater.* **2022**, *32*, 2109772.
[37] W. Zhao, T. Sun, Y. Zheng, Q. Zhang, A. Huang, L. Wang, W. Jiang, *Adv. Sci.* **2022**, *9*, 2201075.
[38] D. Zhao, S. Fabiano, M. Berggren, X. Crispin, *Nat. Commun.* **2017**, *8*, 14214.
[39] Y. Han, J. Zhang, R. Hu, D. Xu, *Sci. Adv.* **2022**, *8*, eabl5318.
[40] M. Jeong, J. Noh, M. Z. Islam, K. Kim, A. Sohn, W. Kim, C. Yu, *Adv. Funct. Mater.* **2021**, *31*, 2011016.
[41] A. Sohn, C. Yu, *Mater Today Phys* **2021**, *19*, 100433.
[42] Z. Liu, H. Cheng, Q. Le, R. Chen, J. Li, J. Ouyang, *Adv. Energy Mater.* **2022**, *12*, 2200858.
[43] Y. Zhao, H. Cheng, Y. Li, J. Rao, S. Yue, Q. Le, Q. Qian, Z. Liu, J. Ouyang, *J. Mater. Chem. A* **2022**, *10*, 4222.
[44] H. Jia, Z. Ju, X. Tao, X. Yao, Y. Wang, *Langmuir* **2017**, *33*, 7600.
[45] K. Liu, J. Lv, G. Fan, B. Wang, Z. Mao, X. Sui, X. Feng, *Adv. Funct. Mater.* **2022**, *32*, 2107105.
[46] Y. Zhao, H. Cheng, Y. Li, J. Rao, S. Yue, Q. Le, Q. Qian, Z. Liu, J. Ouyang, *J. Mater. Chem. A* **2022**, *10*, 4222.
[47] Z. A. Akbar, Y. T. Malik, D.-H. Kim, S. Cho, S.-Y. Jang, J.-W. Jeon, *Small* **2022**, *18*, 2106937.
[48] C.-G. Han, X. Qian, Q. Li, B. Deng, Y. Zhu, Z. Han, W. Zhang, W. Wang, S.-P. Feng, G. Chen, W. Liu, *Science* **2020**, *368*, 1091.

Ya-Hsin Pai graduated with a B.S. in Applied Physics and Chemistry from University of Taipei, Taiwan in 2020. She is currently a graduate student in the group of Prof. Ziqi Liang at Fudan University. Her research area is focused on organic and hybrid thermoelectrics.

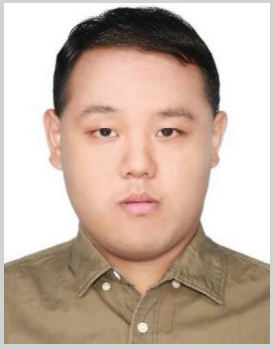

Junhui Tang graduated with a B.S. in Materials Chemistry from Fudan University in 2018. He is currently a Ph.D candidate in the group of Prof. Ziqi Liang at Fudan University. His research area is focused on organic and hybrid thermoelectrics.

Yan Zhao received his B.S. degree in Chemistry from Shandong University in 2008 and a Ph.D. degree in Physical Chemistry from the Institute of Chemistry, Chinese Academy of Sciences (CAS) in 2014. He is now an Associate Professor at Department of Materials Sciences, Fudan University. His research focuses on the processing of organic/polymer semiconductors for field-effect transistors, organic circuits, and organic sensors.

Ziqi Liang obtained his Ph.D. in Polymer Science in the Department of Materials Science and Engineering at Pennsylvania State University in March 2006. He then pursued postdoctoral work at the University of Cambridge from May 2006 to 2008. In June 2008, he joined the National Research Energy Laboratory as a postdoctoral researcher, later to become Scientist III. In September 2012, he joined the Department of Materials Science at Fudan University as a professor. Prof. Liang's group conducts research on organic/perovskite semiconductors-based photovoltaics and thermoelectrics.